Oxygen Electro-Reduction On C22 And C276 Nickel Metal Alloy

S. P. Rogers[a], D. F. Gervasio[a], and J. H. Payer[b]

[a] The Biodesign Institute, Arizona State University, Tempe, Arizona 85287, USA
[b] Department of Materials Science & Engineering, Case Western Reserve University, Cleveland, Ohio 44106, USA

The C22 and C276 alloy metal surfaces were characterized for electrochemical activity in alkaline aqueous media in the presence and absence of oxygen (O_2) and at 30° C. The metal was studied by electrochemical impedance spectroscopy (EIS), voltammetry with a still electrode and a specialized rotating ring-disk electrode (RRDE) technique, the cyclic potential ring measurement (CPRM) method (1). The CPRM method gave the steady state O_2 reduction kinetics. An initial study of O_2 reduction on gold yielded virtually identical results to the work of Vilambi and Taylor who first described the CPRM method. The application of the CPRM method to the study of O_2 reduction on C22 and C276 showed strong evidence for a predominantly series 2 step, 2 electron O_2 reduction pathway, where kinetic rate constants k_2 (evaluated at -0.7V versus the saturated calomel electrode) and k_3 (evaluated at -1.2V) were estimated at 30° C to be 0.001 cm/s and 0.193 cm/s respectively for C22 and 0.013 cm/s and 0.232 cm/s respectively for C276.

Introduction

Oxygen (O_2) reduction is the most likely process that sustains metal oxidation in air. This occurs through electrochemical "local cells" on the metal surface, where oxygen reduction occurs at one localized metal surface site by accepting electrons generated during metal oxidation occurring at another localized site through electron conduction in the bulk metal underlying both sites. Oxygen reduction sites become alkaline and metal oxidation sites become acidic. Significant metal loss occurs when this electrochemical corrosion occurs unchecked, but is arrested when O_2 reduction is arrested; a process often called "cathodic stifling". Oxygen reduction on C22 and C276, two nickel-chromium-molybdenum (Ni-Cr-Mo) alloys, was in cells containing aqueous potassium hydroxide (KOH) solution to simulate O_2 reduction on metal surfaces covered by thin layers of moisture, where the cathodic solutions are likely to become more alkaline. The findings are part of an overall study of local corrosion cells on the surface of C22 and C276 alloys, and provide experimental inputs to computational methods for predicting the corrosion processes, such as pitting, crevice corrosion, stress corrosion cracking, and galvanic action. In particular, the objectives were to establish whether O_2 reduction does occur on nickel metal alloy, to examine the conditions under which it does occur, and to measure the kinetics for O_2 reduction.

Previous studies of O_2 reduction on steel alloy by the co-authors (2) using the cyclic potential ring measurement (CPRM) method described by Vilambi and Taylor (1), showed evidence for a series 2 step, 2 electron pathway for O_2 reduction to water, and

estimated the rate constants, k_2 and k_3, for this mechanism. This mechanism has been described by Wroblowa, *et. al.* (3) and Zecevic, *et. al.* (4), shown below in Figure 1, and was scrutinized by Yeager (5). In the scheme, O_2 can receive 4 electrons to directly form
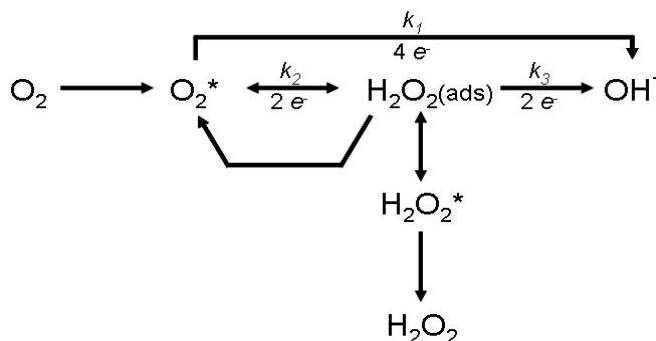

Figure 1. In neutral solutions, the general scheme for O_2 reduction.

2 waters, described by rate constant k_1 (direct pathway) or can receive 2 electrons in a sequential 2 step pathway (series pathway) described by k_2 to form peroxide then 2 waters as described by k_3. Obviously, O_2 reduction can proceed by the two pathways simultaneously (parallel pathway) and be described by linear combinations of k_1, k_2, and k_3. The CPRM method is a specialized rotating ring-disk electrode (RRDE) technique where the same detection activity on the gold (Au) ring is maintained by continually cycling the ring over a small potential range, typically in the oxidizing potential regime. The ring, in effect, detects reduced species generated at the disc. We report the quantitative detection at the Au ring of peroxide formation due to O_2 reduction on nickel metal alloy discs, C22 and C276. From the O_2 reduction currents at the nickel metal alloy discs and peroxide oxidation currents at the gold ring, we show strong evidence for the series 2 step O_2 pathway and were able to estimate the rate constants k_2 and k_3 at 30° C.

Experimental

General Approach for All Experiments

Stock electrolyte solutions were prepared with ultra pure de-ionized water (18.2 MΩcm conductivity, PureLab Ultra system) and KOH pellets (Mallinckodt AR® ACS grade) to a concentration of 1 mole KOH per 1 liter of water (1<u>M</u>), stored in Teflon® containers, and allowed to equilibrate over night. The pH was measured using color**pH**ast® indicating strips (EM Science), with a resolution of 0.5 pH units over a pH range of 7.5 – 14. The electrolyte was volumetrically transferred, 100 ml, to a single compartment, 5 neck, jacketed Pyrex® vessel configured with a shielded glass stopcock reference electrode bridge with Luggin tube tip separating the electrolyte in the vessel from a Saturated Calomel reference electrode (0.2446V vs. NHE). A spectroscopic grade (99.999%) graphite rod was used as the auxiliary electrode. The electrolyte and vessel ambient were equilibrated with either ultra pure argon (Ar) or O_2 by sparging through a medium glass fritted tube for a minimum of 30 minutes. Electrode potentials and current acquisitions were controlled by a Princeton Applied Research VMP2 Multichannel Potentiostat (Oak Ridge, TN) running EC-Lab version 9.13 software. The electrolyte

was thermostatted by circulating water/glycol through a thermostatic bath at 30° C ± 1° C to the jacketed Pyrex® vessel.

Still Solution Voltammetry and EIS

The working electrode was C22 or C276 (Corrosion Materials Inc., Baker, LA) Ni-Cr-Mo alloy rod stock cut to 15.24 cm (6") long x 0.16 cm (1/16") outside dimension (o.d.) The electrode was dry abraded with 400 and 600 grit silicon carbide (SiC) paper; wiped between abrades with dry Kimwipe tissue and prior to placement in electrolyte. The working surface area was ≈ 1.286 cm^2 as determined by marking the rod's position in the electrolyte (≈ 1"). The electrolyte was sparged with either Ar or O_2 for a minimum of 1 hour before admitting the working electrode, pretreated at -1.0V for 5 min., then cycled or ramped at 10 mV/s to -0.6V (vs. SCE) and held for 1 hour prior to EIS studies. The working potential window for cyclic voltammetry (CV) was -0.6V to 0.412V vs. SCE; scanned at 10 mV/s. The EIS parameters were 200 kHz to 10 mHz, with a 20mV$_{pp}$ perturbation.

RRDE Voltammetry

The rotating ring-disk electrode was a Pine Instruments (Raleigh, NC) model AFMTI34DC Au T probe configured with a Au ring (i.d. = 0.75 cm; o.d. = 0.85 cm) and interchangeable disk capability, fitted with a 0.4 cm long x 0.6 cm o.d. disk of C22 or C276 (Haynes International, Kokomo, IN). The collection efficiency of the ring used in this work was that reported by the manufacturer, 0.23, based on disc and ring geometry. The RRDE was prepared by initially planarizing the probe on an 8 inch semi-automated polishing table with successively finer grades wet SiC paper (600, 800, 1200, 2400 grit), followed by successively finer grades wet alumina paper (1, 0.3, 0.05 micrometer, μm). The surfaces of the ring and disc were hand polished to a mirror finish using a wet felt pad and successively finer grades of Buehler (Lake Bluff, IL) alumina slurries (1, 0.5, 0.05 μm), then rinsed with sonication in 95% ethanol followed by ultra pure de-ionized water. Prior to an experimental measurement, the RRDE was buffed using a wet felt pad and 0.05 μm alumina slurry while rotating on a Pine Instruments AFMSRX rotator with MSRX speed controller at 900 rotations per minute (rpm), rinsed in 95% ethanol followed by ultra pure de-ionized water, then immediately positioned in the electrolyte which was previously de-aerated with Ar. The disc was pretreated *in situ* prior to the CPRM procedure described below at -1.3V for 5 minutes to what will be referred to throughout this writing as a "pristine" metal surface.

Cyclic Potential Ring Measurement (CPRM) Methods. The CPRM procedure using a Au-Au RRDE for data collection at each disc hold potential is shown in Figure 2 as a 2 step sequence of timed events. First in an Ar de-aerated environment, the "pristine" metal disc was equilibrated at a hold potential in the range of 0.0V to -1.5V (-0.7V in the Figure 2 example) for 13 minutes at 4900 rpm. The Au ring was activated or "cleaned" by cycling the ring over the potential range of -1.5V to 0.7V at 500 mV/s for 1 minute (14 cycles) starting at the 11 minute mark. The Au ring was scanned after the ring "cleaning" over a potential range of -0.25V to 0.7V at 500 mV/s for 1 minute (16 cycles) for each of the rotation rates listed at the bottom of Figure 2, (4900, 900, 2500, 3600, 1600, and 4900 rpm) with a 1 minute stabilization period. During the rotation rate stabilization period, disc current data was acquired from a 30 second average of disc current prior to the ring
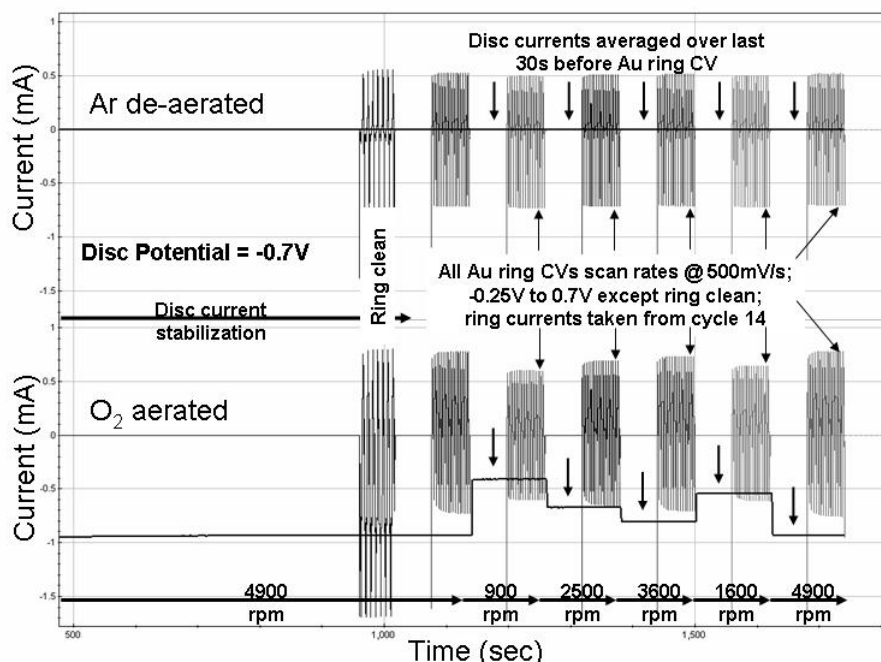
Figure 2. The CPRM procedure using a Au-Au RRDE for data acquisition at a disc hold potential, -0.7V in this example.

cycling event. Ring current data was taken from only cycle 14 and averaged over the potential range of 0.5V to 0.6V. This same CPRM procedure was repeated (second step) after the Au-Au RRDE was brought back to a "pristine" metal condition and the disc stabilized at the same potential in an O_2 saturated environment. The disc and ring currents were acquired in exactly the same manner, at the same time and rotation rate sequence. This exact procedure was repeated for Au disc hold potentials from 0.0V to -1.5V in 0.1V step increments.

The CPRM procedure using a Au-Ni alloy RRDE for data collection at each disc hold potential is shown in Figure 3, as a single step sequence of timed events. This procedure was simplified from the previous CPRM procedure using a Au-Au RRDE. Only one disc and one ring background current was acquired at 4900 rpm, since there was very little to no difference in the background currents of the ring and disc in an Ar de-aerated condition between all of the rotation rates. In this procedure, the "pristine" metal disc was stabilized at a potential in Ar de-aerated environment for the single background current determination and continued to be held at that potential during the gas exchange to an O_2 saturated environment. Disc and ring current were acquired in the O_2 saturated environment in the same manner as previously described for the time and hydrodynamic conditions shown in Figure 3. This procedure was repeated for the Ni-Cr-Mo alloy discs C22 and C276 held at potentials from 0.0V to -1.5V in 0.1V step increments.

Results

Still Solution Voltammetry and EIS

Figures 4a and 4b show the cyclic voltammetry of C22 in alkaline water in Ar de-aerated and O_2 saturated environments respectively. The overall scan profile was similar
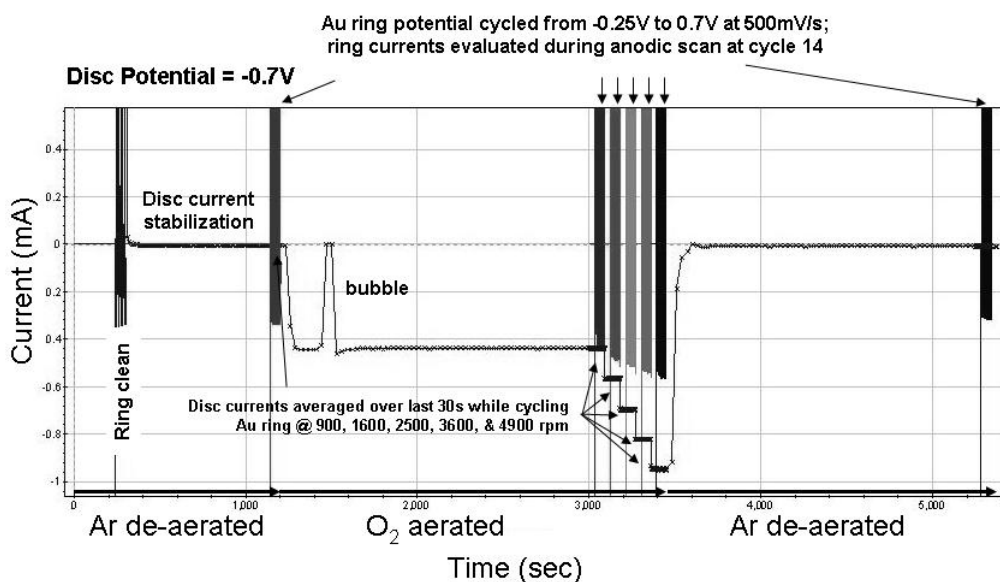
Figure 3. The simplified CPRM procedure using a Au-Ni alloy RRDE for data acquisition at a disc hold potential, -0.7V in this example.
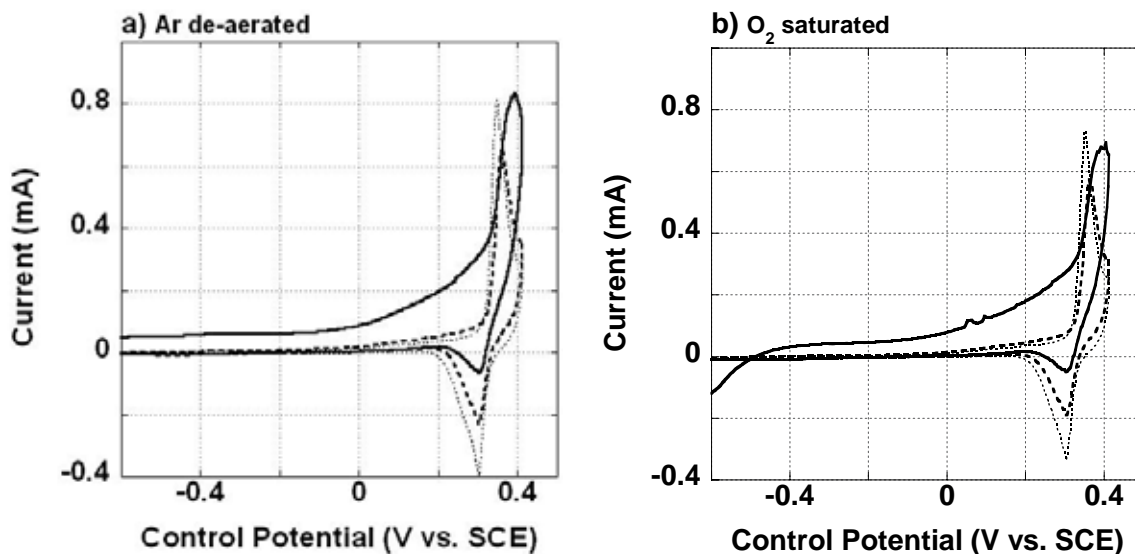

Figure 4. Cyclic voltammetry scanned at 10mV/s recorded for C22 alloy (rod ~ 1.29 cm^2) at 30°C equilibrated in a) Ar de-aerated and b) O_2 saturated, 1$\underline{M}$ KOH electrolyte at pH 14. The currents for each of the scan cycles are integrated for plot a) Ar de-aerated: cycle 1 (▬), i_{ox} = 14.15mC and i_{red} = 1.33mC; cycle 2 (– – –), i_{ox} = 5.15C and i_{red} = -0.90mC; cycle 3 ($\cdots$), i_{ox} = 5.19mC and i_{red} = -2.52mC; and for plot b) O_2 saturated: cycle 1(▬), i_{ox} = 10.75mC and i_{red} = 1.04mC; cycle 2(– – –), i_{ox} = 4.30mC and i_{red} = -0.89mC; cycle 3 ($\cdots$), i_{ox} = 4.58mC and i_{red} = -2.14mC.

to that reported by Lloyd, *et. al.* (6) in acidic electrolyte with a shift of ~ 60mV/pH unit. The first negative to positive potential polarization cycle always showed a extra anodic current from –0.6V to 0.4V, indicative of an predominately metallic surface (M^0) being oxidized to form a predominately metal oxide surface layer with oxidation peaking at ~

0.4V. The reverse positive to negative potential scan showed a reduction peak between 0.35V and 0.25V. The second and successive cycles showed growing oxidation (0.3V to 0.38V) and reduction peaks. After the second polarization cycle, the cathodic current seemed to increase at a greater rate than the anodic current. Similar results were found for the C276 metal alloy.

Figure 5 shows electrochemical impedance spectra (EIS) for Alloy C22 in 1$\underline{\text{M}}$ KOH electrolyte equilibrated in a) Ar de-aerated and b) O_2 saturated environments at 30°C.
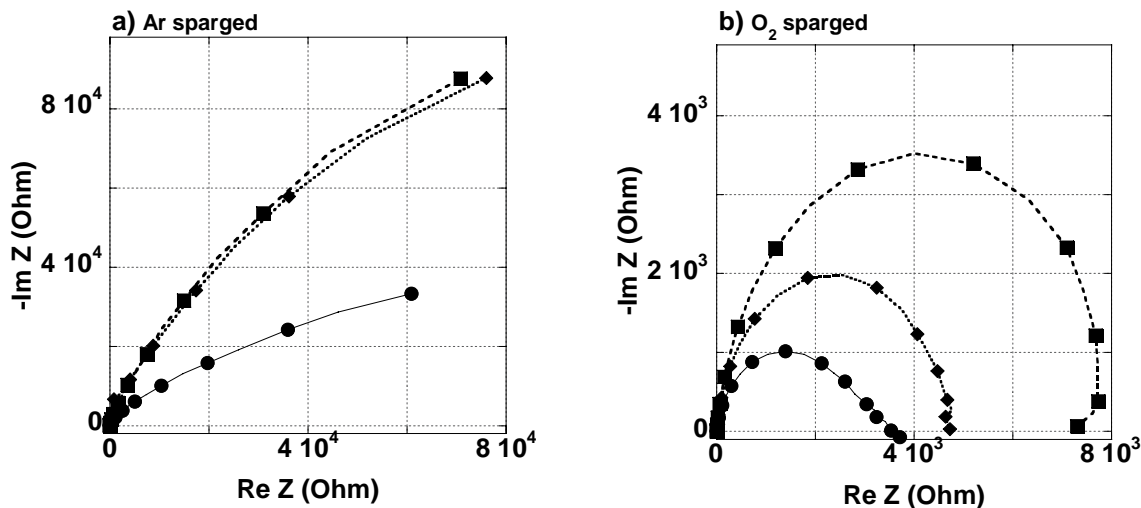

Figure 5. Electrochemical Impedance Spectra (EIS) for C22 (A= 1.29 cm^2) in a) Ar de-aerated and b) O_2 saturated environments, 1$\underline{\text{M}}$ KOH electrolyte at 30°C and pH 14. The Ni rod was abraded, held at -1.0V for 5min, ramped at 10mV/s to -0.6V, aged at that potential; EIS at -0.6V with 20mV perturbation. (● – 0hr aging; ■ – 1hr aging; ♦ -16hr aging)

After the impedance measurements under O_2, the electrolyte was sparged with Ar for at least 1 hour, and without removing the Ni rod, before the EIS experiment was repeated. The exception was the no aging at -0.6V experiment, where the Ni rod was removed and freshly abraded. Under Ar, there is a very large ascending arc that does not form a semicircle as far out as 80,000 Ohms on the real axis when the slowest oscillation is 10 mHz. But under O_2, a full semicircle is seen intercepting the real axis at 3,600, 4,900 and 7,900 Ohm when the electrode was held at -0.6V for 0, 15 and 1 hours, respectively. Clearly the forming of these 3 semicircles was due to O_2 charge transfer resistance on C22 in this alkaline electrolyte. It appears metal oxide reduction slowly occurs at -0.6V resulting in a less resistive passivation film as the oxygen reduction kinetics actually get faster (semicircle is smaller) after holding at -0.6V for 16 hours compared to 1 hour, but the smallest semicircle is when there was no aging.

RRDE Voltammetry and CPRM

Cyclic voltammetry survey scans were acquired over a potential range of -1.5V to 0.7V for the Au, Alloy C22, and Alloy C276 electrode materials used in the RRDE for CPRM experiments. Figure 6 shows survey scans for these RRDE materials which are the same as metal foil and rod materials in still solutions. Little or no slope is evident in

the plots about the 0 mA current region, indicating a proper sealing of the probe electrode materials, and defining the geometric surface areas for the Au ring and Alloy C22 and C276 discs. In Figure 6b, the CV for Alloys C22 and C276 are very similar, and C22 shows greater oxidation and reduction currents than C276.
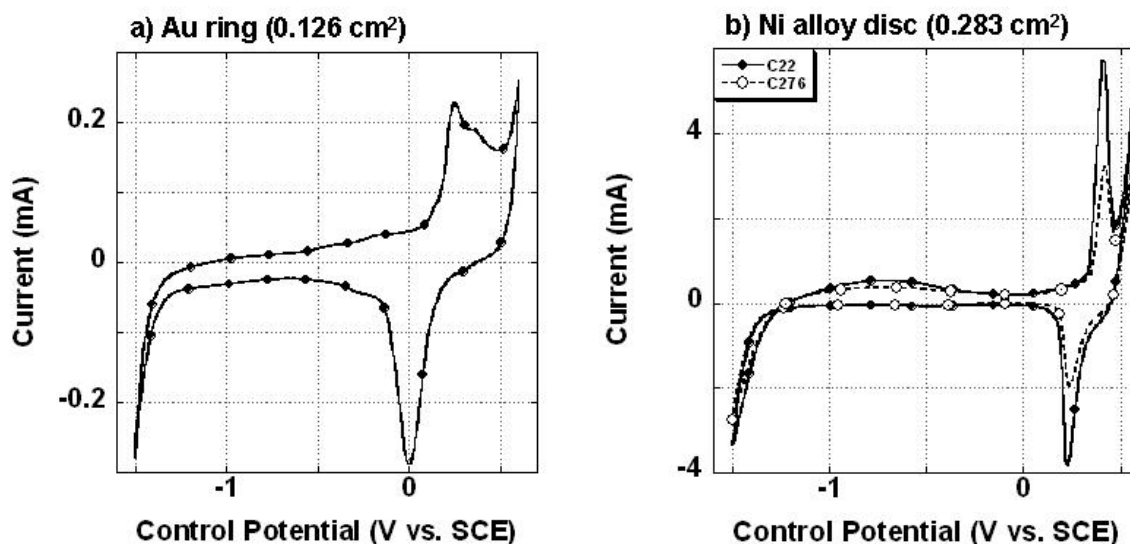

Figure 6. Cyclic voltammetry potential range survey scans for the a) Au ring and b) Alloys C22 and C276 discs used in the CPRM method: Ar de-aerated 1$\underline{M}$ KOH @ 30°C, pH = 14, 500mV/s scan rate, 4900 rpm, 6th cycle.

The CPRM procedure depicted in Figure 2 using Au-Au RRDE was repeated on pristine metal for each disc potential step, in 0.1V steps, from 0.0V to -1.5V, and the ring and disc current results are shown in Figure 7 for the rotation rates 900, 1600, 2500, 3600, and 4900 rpm. Each of the data points in the ring current plot was the averaged current acquired on cycle 14 between 0.5V to 0.6V, where the "background" current from the Ar de-aerated experiment was subtracted from the O_2 reduction current in the O_2 saturated experiment. Similarly, each of the data points in the disc current plot was the averaged current acquired over a 30 second period at the hold potential just prior to the ring cycling event. After normalizing for the disc area and correcting for the reference electrode potentials, the comparison of our CPRM results for O_2 reduction to Vilambi & Taylor's original work (1) of the CPRM results for their O_2 reduction on Au are virtually identical. It is noted at this point and will be emphasized later, that one of the conclusions in Vilambi & Taylor's CPRM work on Au-Au RRDE was O_2 reduction was a 2 step process. Two limiting current plateaus are evident in the Au disc current plot (bottom) in Figure 7.

Application of the precise CPRM procedure shown in Figure 4 at -0.7V was repeated for 0.1V step disc hold potentials from 0.0V to -1.5V, where Alloys C22 and C276 were brought to "pristine" metal prior to each potential step is shown in Figure 8a for Alloy C22 and Figure 8b for Alloy C276. Again, each of the data points in the ring current plots (top) was the current average acquired on cycle 14 between 0.5V to 0.6V, and the "background" current from the Ar de-aerated step at 4900 rpm was subtracted from each the O_2 reduction currents acquired at the rotation rates listed in Figure 3 during the O_2 saturation step. The disc currents at each of the hold potential steps were averaged over
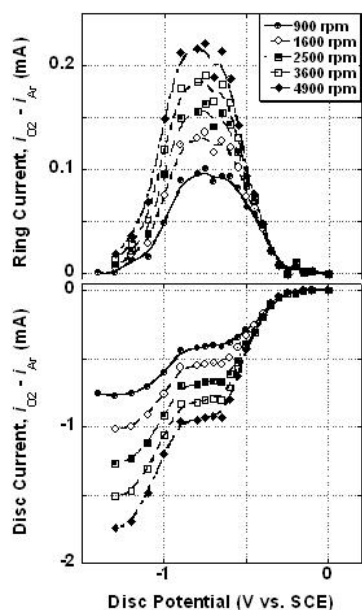
Figure 7. Au ring (top, 0.126 cm^2) and Au disc (bottom, 0.283 cm^2) polarization data for O$_2$ reduction using the CPRM method in 1$\underline{\text{M}}$ KOH at 30° C, and pH 14.

the last 30 seconds during the ring cycling event for that rotation rate. There is evidence of only one limiting current plateau in the disc current plots (bottom) for O$_2$ reduction on C22 and C276.

Bubble formation was observed for disc hold potentials at -1.2V and more negative. The resulting reduction in surface area due to bubbles adhering to the ring and disc surfaces corrupted current determinations in this potential region. Figure 6a and 6b shows this potential region to be the region for hydrogen generation for both Au and Alloys C22 and C276. Comparing the ring currents (top) in Figure 8 for the maximum current detected for O$_2$ reduction, there is ~ 0.1V difference for peroxide (H$_2$O$_2$) formation on C22 vs. C276.

Discussion

As shown in TABLE I, Alloys C22 and C276 have similar nickel (Ni) compositions and differ in weight percent (wt%) of alloying elements cobalt (Co), chromium (Cr), iron (Fe), molybdenum (Mo), and tungsten (W). It is not surprising there is little difference in the voltammetry for the two nickel alloys (Figure 6b). However, it is presumed elemental alloy composition plays a role in physical and chemical properties of the metal, as may be evident in the oxide growth observed on Alloy C22 in Figure 4b. The voltammetry window, as shown in Figure 6, was limited by reduction of water protons at approximately -1.3V and water oxidation at about 0.6V versus SCE.

TABLE I. Nickel Alloy wt% Composition (7).

Ni Alloy	Co	Cr	Fe	Mn	Mo	Ni	Si	V	W
C22	0.72	21.00	3.90	0.23	13.30	57.94	<0.03	0.01	2.90
C276	1.45	15.74	5.58	0.50	15.53	57.57	0.02	0.16	3.45

Vilambi and Taylor's CPRM O$_2$ reduction study on Au had shown a 2 electron, 2 step series pathway, primarily by accounting for 100% of the Au disc current due to peroxide formation. We repeated this study with the same results, obtaining limiting current data that was linear in accordance with the Levich relation (8) and accounted for 100% of the disc current due to H$_2$O$_2$ formation. Ring currents corrected with the RRDE collection coefficient which yield less than the disc current can be attributed to parallel O$_2$ reduction pathways. Using the CPRM methodology and as Gervasio and Payer had done previously (2), the kinetics for O$_2$ reduction on nickel metal alloys was investigated in the same way. However, there was no evidence (Figure 8) for a second limiting current associated with

H_2O_2 reduction to H_2O. The limiting current due to H_2O_2 reduction to H_2O was estimated as twice the limiting current for O_2 reduction to H_2O_2, and justified experimentally.
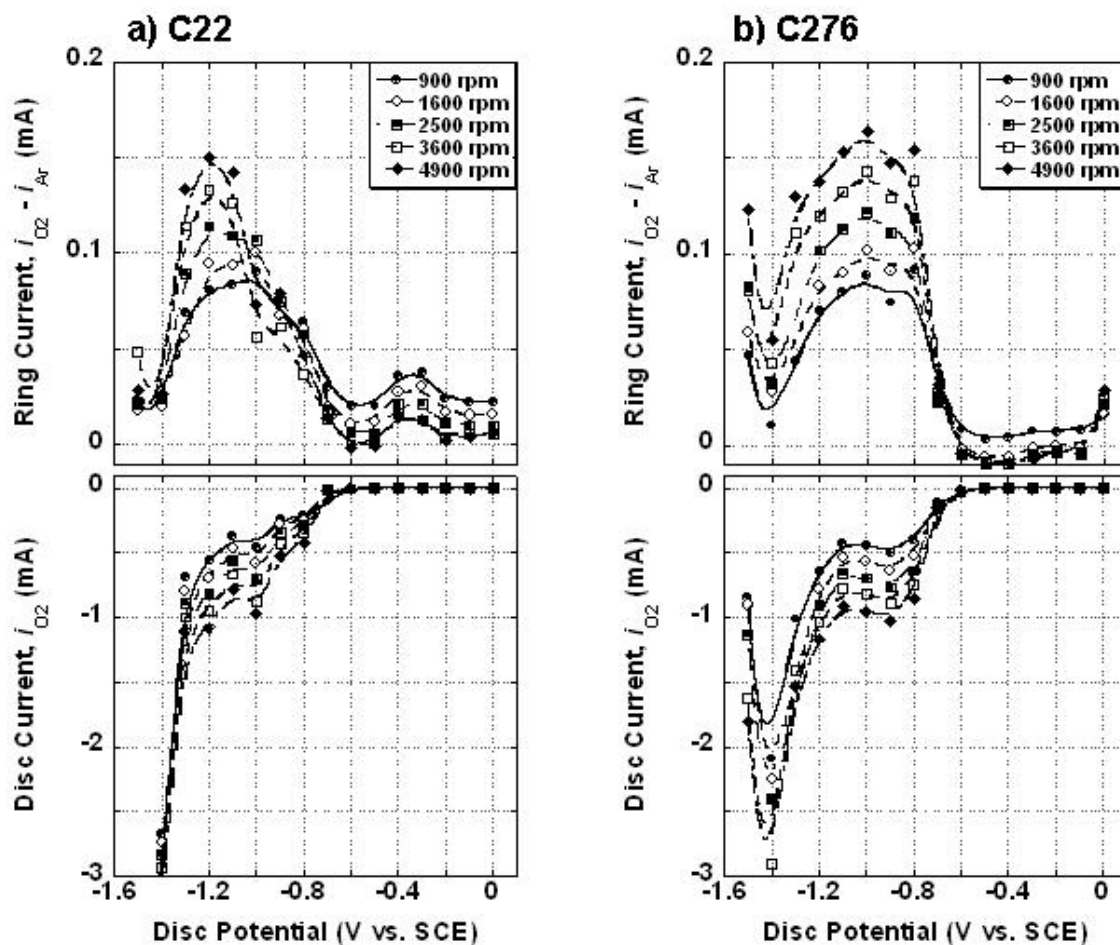

Figure 8. CPRM plots for O_2 reduction on Alloy a) C22 and Alloy b) C276 in 1$\underline{M}$ KOH @ 30°C and pH = 14. The Au ring area is 0.126 cm^2 and Alloy C22 and Alloy C276 discs are 0.283 cm^2.

To justify this approximation, disc currents were acquired at 0.1V step potentials over the range of 0.0V to -1.5V on C276 rotating at 2500 rpm in 1$\underline{M}$ KOH (30°C and pH 14) equilibrated first in an Ar de-aerated environment, followed by the acquisition of disc currents on C276 in exactly the same manner, over the same potential range, in an Ar de-aerated environment with 16 m$\underline{M}$ reagent H_2O_2 addition to the 1$\underline{M}$ KOH electrolyte (30°C and pH 14). Figure 9 plots the C276 disc currents with and without the reagent H_2O_2 addition to the 1$\underline{M}$ KOH electrolyte in an Ar de-aerated environment along with the previously acquired O_2 reduction CPRM data at 2500 rpm for C276. In Figure 9, the solid line and circles shows the ring and disc currents for O_2 reduction on C276. The small grey dashes and open circles is the C276 disc current in an Ar environment showing a reduction onset current occurring at -1.2V and continues with no limiting current plateau. The large grey dashed line with solid squares is the disc current due to H_2O_2 reduction on C276 with on onset at about -1.0V, which correlates well with the maximum H_2O_2 formation for O_2 reduction on C276. The small reduction onset current at -0.6V is believed to be disproportionation of H_2O_2 at the relatively high concentration used in the

experiment. Again, no limiting current plateau was observed due to the concurrent reduction of proton to hydrogen. The results shown in Figure 9 showing only one reduction onset current observed for reagent H_2O_2 reduction in an Ar de-aerated environment, and the application of the ring collection coefficient accounting for 90% to 100% of the disc current due to H_2O_2 formation, strongly indicates a series 2 step pathway for O_2 reduction on Alloys C22 and C276.
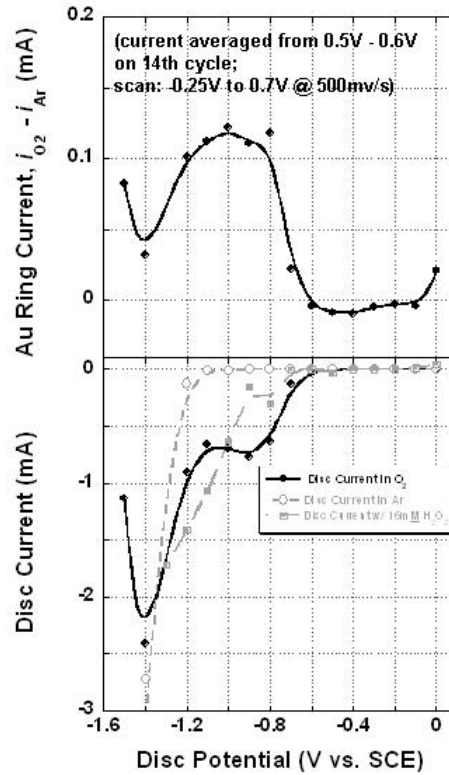

Figure 9. Experimental evidence for a 2 step series O_2 reduction pathway on nickel alloy using H_2O_2 reagent added to 1M KOH @ 30°C and pH = 14. (See text for details.)

The kinetic current can be obtained from the steady state disc data by calculating according to expression [1], where j_L is the limiting current density and j is the current density. An estimate of the rate constant, k_{exp}, for peroxide and water generation can be made by considering first the rate of O_2 electro-reduction reaction on Alloys C22 and C276 in alkaline media should have a first order dependence on O_2 concentration (9), expression [2], and second that the concentration of O_2 in aqueous 1M KOH equilibrated with 1 atmosphere of O_2 over solution is 2.2 x 10^4 moles per liter (10). The first wave of

$$j_{kinetic} = j_L \, j/(j_L\text{-}j) \qquad\qquad [1]$$

$$j_{kinetic} = k_{exp}n[O_2]^1 \qquad\qquad [2]$$

O_2 reduction on Alloys C22 and C276 between -0.6 to -1.0V vs. SCE goes to peroxide formation; an n value of 2 can be used along with the kinetic current determination from expression [1] to give k_{exp}, which should be the same as k_2 in Figure 1, the rate constant for peroxide generation. The value of k_2 calculated in this way is roughly, 0.001 cm/s for

C22 and 0.013 cm/s for C276. Figure 10 plots k_2 and k_3, calculated as stated above, as a function of Alloy C22 and C276 disc potential.
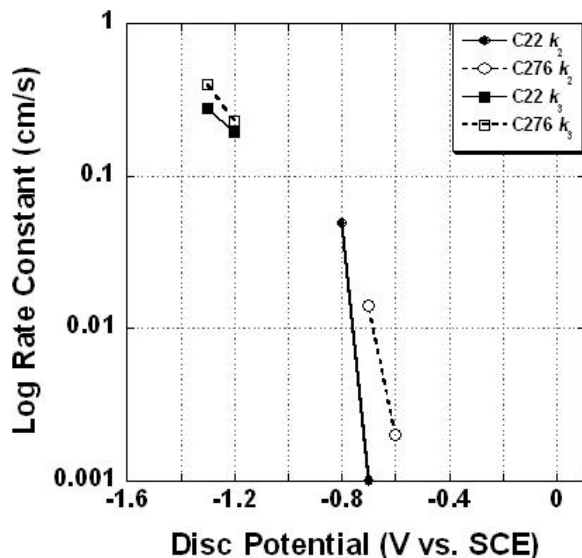

Figure 10. Estimated rate constants, k2 and k3 for H2O2 and H2O formation, respectively, on Alloy C22 and Alloy C276 for a given potential.

Summary and Conclusions

The voltammetry under Ar and O_2 suggested accumulation of oxide on C22 and C276 with successive scans between –0.6V and 0.4V vs. SCE. Oxygen reduction was occurring in oxygenated solution, as suggested by the clear suppression of oxidation current in the voltammetry under oxygen compared to Ar, and the formation of a full semi circle in the Nyquist plots under O_2 but no semicircle formation in the EIS under Ar. Repeating Vilambi and Taylor's CPRM O_2 reduction on Au-Au RRDE provided a benchmark to study O_2 reduction on Alloys C22 and C276 using a Au-Alloy C22 and Au-Alloy 276 RRDE. The onset potential for O_2 reduction on C22 and C276 in alkaline water, at 30° C and pH 14, was approximately -0.6V and continued to -1.5V (vs. SCE). The use a RRDE and the CPRM method was, at the very least, a semi-quantitative approach that showed strong evidence for a series 2 step, 2 electron pathway for O_2 reduction on nickel metal alloys where the rate constants, k_2 and k_3, were estimated, even with the ill-defined limiting current for peroxide reduction to water. The rate constants, k_2 (@ -0.7V for O_2 to H_2O_2) and k_3 (@ -1.2V for H_2O_2 to H_2O), were estimated to be 0.001 and 0.013 cm/s, respectively, for C22 and 0.193 and 0.232 cm/s, respectively, for C276.

Acknowledgments

recommendations of authors expressed herein do not necessarily state or reflect those of the DOE/OCRWM/OCS.

References

1. N. R. K. Vilambi and E. J. Taylor, *J. Electrochem. Soc.*, **270**, 61 (1989).
2. D. Gervasio and J. H. Payer, in *Fundamental Understanding of Electrode Processes in Memory of Professor Ernest B. Yeager*, J. Prakash, D. Scherson, M. Enayetullah, and I.-T. Bae, Editors, p. 58, Proceedings of the Electrochemical Society, Orlando, FL (2003).
3. H. S. Wroblowa, Y. D. Pan, and G. Razumney, *J. Electroanal. Chem.*, **60**, 195 (1976).
4. S. Zecevic, D. Drazic and S. Gojkovic, *J. Electroanal. Chem.*, **265**, 179 (1989).
5. E. Yeager, *J. Electrochim. Acta.*, **29**, 1527 (1984).
6. A. C. Lloyd, D. W. Shoesmith, N. S. McIntyre, and J. J. Noël, *J. Electrochem. Soc.* **150**, (4) B121 (2003).
7. *C22 and C276 Alloy Certification of Tests*, Haynes International Inc., supplied with material.
8. V. G. Levich, *Physico-Chemical Hydrodynamcs*, Prentice Hall, Englewood Cliffs, NJ, (1962).
9. V. Jovancicevic, and J. O'M. Bockris, *J. Electrochem. Soc.*, **133**, 1797 (1986).
10. D.B. Radtke, A.F. White, J.V. Davis, and F.D. Wilde, "6.2 Dissolve Oxygen" in U. S. Geological Survey TWRI, Book 9, 26 (April, 1998).